Desalination and Water Treatment
www.deswater.com

doi: 10.1080/19443994.2013.792007

52 (2014) 1885–1894
February

Taylor & Francis
Taylor & Francis Group

Molecularly imprinted polystyrene-divinylbenzene adsorbents for removal of bisphenol A

Katri Laatikainen[a,*], Marek Bryjak[b], Markku Laatikainen[c], Heli Sirén[a]

[a]*Laboratory of Chemistry, Department of Chemical Technology, Lappeenranta University of Technology, P.O. Box 20, FI-53851 Lappeenranta, Finland*
Tel. +358 40 1823138; Fax: +358 5 621 2199; email: katri.laatikainen@lut.fi
[b]*Faculty of Chemistry, Department of Polymer and Carbon Materials, Wroclaw University of Technology, 50-370 Wroclaw, Poland*
[c]*Laboratory of Industrial Chemistry, Department of Chemical Technology, Lappeenranta University of Technology, P.O. Box 20, FI-53851 Lappeenranta, Finland*

Received 19 October 2012; Accepted 21 March 2013

ABSTRACT

The effect of acrylonitrile co-polymerization and molecular imprinting on bisphenol A (BPA) affinity by the polystyrene-divinylbenzene adsorbents was studied. Adsorption equilibria were measured using batch uptake experiments and equilibrium data were analyzed by means of Langmuir isotherm and Scatchard approach. The calculated parameters were utilized for modeling of adsorption–microfiltration hybrid system. The highest BPA capacity, 27 mg/g, is achieved for the material synthesized with 10% BPA template concentration in relation to monomer. Acrylonitrile does not improve BPA affinity or adsorption capacities of sorbents. BPA sorption rate can be described assuming pore diffusion control and using a tortuosity factor of 3. The estimated equilibrium and mass transport parameters describe reasonably well the removal of BPA in the adsorption–microfiltration hybrid system. Model calculations show that 97% reduction in BPA concentration is attained with sufficiently high amount of the adsorbent.

Keywords: Molecularly imprinted polymer; Polystyrene-divinylbenzene; Adsorption; Bisphenol A; Adsorption-membrane hybrid system

1. Introduction

Many chemicals present in the environment can affect endocrine systems and produce an adverse effect on aquatic life, wild animals and probably on human beings. These pollutants are called endocrine disrupting compounds (EDCs). Among the EDCs, estrogenic compounds are the main problem. One of the most dangerous estrogenic compounds in water is bisphenol A (BPA). It is monomer from which can be made by polymerization of polycabonates, polysulfones and epoxy resins [1]. Moreover, it has been used as coatings on cans, powder paints, additives in thermal paper, in dental fillings, and antioxidants in plastics [2]. It has been reported that even the very low concentrations of BPA can affect the reproduction and development systems of organism and make serious problems for human and animals [3]. BPA is released into the environment during manufacturing processes

---

*Corresponding author.

and by leaching from final products [4]. According to Markey [5], a slight amount of BPA is eluted from plastic packages and pollutes food, and drinks.

Because BPA is inherently hydrophobic, adsorption is one of the suitable processes for the removal of it from waste waters [6]. Removal of BPA from waters using activated carbon has been widely studied [7–9]. During the last decade, materials with higher recognition and selectivity have been studied intensively [1,3,6,10,11].

Molecular imprinting technique is a synthetic method, which offers solution for preparation of separation materials with extremely high selectivity. Principle of molecular imprinting is shown in Fig. 1. This technique combines the binding ability of functional groups or ligands for target substrates with shape- and size-selective cavities imprinted into the structure of a rigid solid material [12]. Molecular imprinting has been mainly used in biochemical applications such as microreactors, immunoassays and antibodymimics, catalysis, artificial enzymes, and bio- and chemo-sensors [13]. It has been also used in several analytical techniques, for instance in liquid chromatography [14,15], capillary electrophoresis and capillary electrochromatography [16], solid phase extraction [17], and sensor technology [18].

Molecular imprinted polymers (MIP) and the adsorbents or membranes based on specific functionality seem to be suitable for the selective separation of e.g. estrogenic compounds, because their phenolic groups make molecular recognition easier [6]. The basic idea of MIPs, also called as artificial receptors, is based on formation of selective binding sites during polymerisation by using suitable functional monomers and the target compound as template. Reusability of the adsorbent is also important because of economical and environmental aspects and, therefore, compromise between strong binding and regenerability has to be found. Although MIP materials used for the removal of BPA have been widely studied [1,3,4,10], adsorption capacity of the materials is not high, and also binding kinetics is quite slow [1,3]. On the other hand, activated carbons have high capacity but the selectivity is the determining issue.

Conventional separation systems operate with particle size of 250–1,000 µm. Smaller particles tend to block the column and with very large particles, kinetics is too slow. At any rate, feed flow rates which can be used are so slow that ion exchange and adsorption can be economically used only in a limited number of applications. Instead of fixed-bed system, an alternative separation process is provided by combining ion

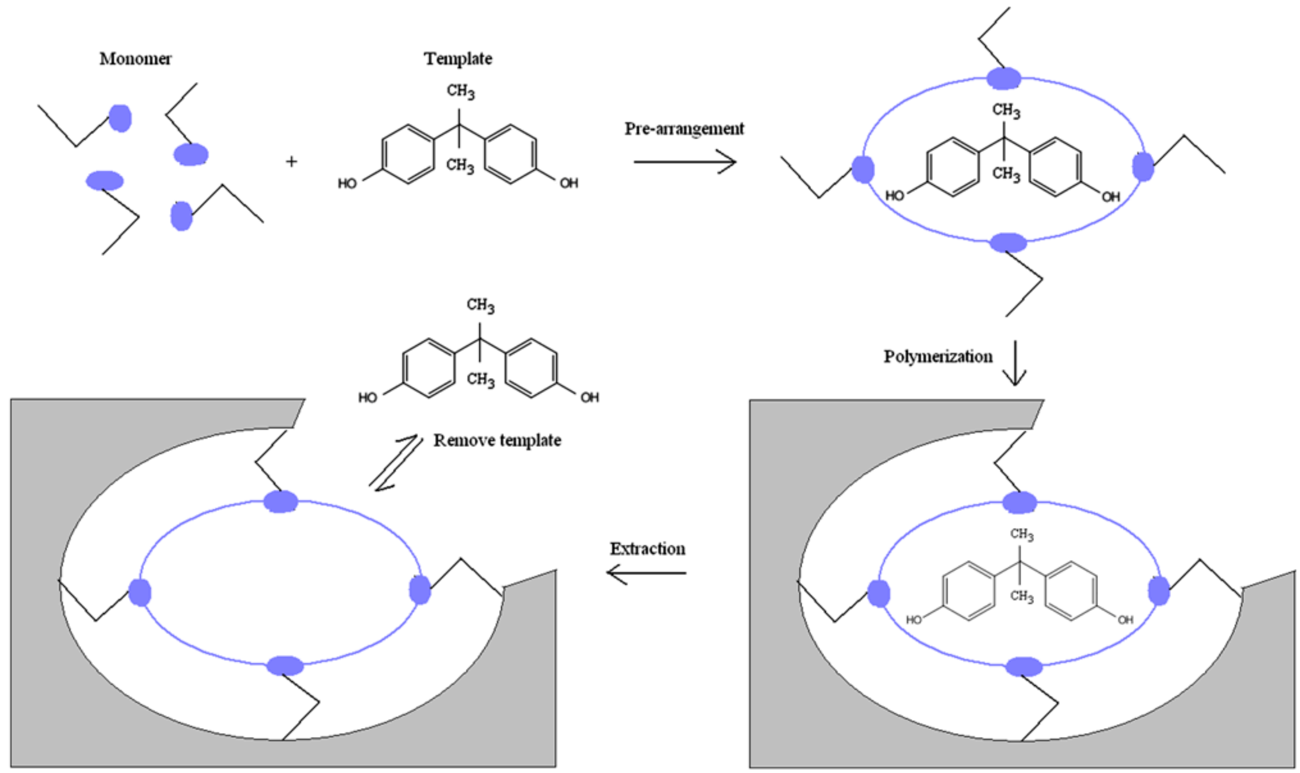

Fig. 1. Principle of molecular imprinting (MIP) technique.

exchange or adsorption with membrane techniques. This technique is called adsorption-membrane hybrid system [19] and its advantages are: (1) particle size can be much smaller than in the case of column separation system, (2) energy consumption is not as high as in the fixed-bed mode, and (3) some synergetic effects that may appear at the membrane surface can cause intensification of the process. Adsorption-membrane hybrid system has been studied for removal of organics from waste waters [20], however, the hybrid technique is still in stage of development.

This study is the continuation of our previous work related to use of molecular imprinted membranes for the removal of BPA [21]. The positive effect of polar groups on improvement of BPA sorption by hydrophobic membrane was shown there. The objective of this study is to evaluate BPA adsorption on MIP sorbents prepared from hydrophobic monomers styrene (STY) and divinylbenzene (DVB), and partly hydrophilic monomer acrylonitrile (AN). An idea is to add AN to the STY-DVB matrix to make specific interactions with BPA and to improve sorbent selectivity. AN is easily hydrolyzed to carboxylic groups and can serve as the precursor for them. For this purpose, sorbents with different STY and AN contents were prepared and characterized in the equilibrium conditions. Furthermore, the objective of this study is to use adsorption–microfiltration hybrid system in the removal of BPA by our new synthesized molecular imprinted materials instead of more common column separation system. Adsorption equilibria and kinetics were measured using batch uptake experiments. Equilibrium and kinetic data were correlated with the Langmuir equation and a pore-diffusion model, respectively. Finally, the adsorption–microfiltration hybrid system were modeled using a non-steady model reported recently [22].

2. Experimental section

2.1. Materials

BPA ($C1_5H_{16}O2$, CAS 80-05-7, molar mass 228.29 g/mol) (BPA) (>99%), STY ($\geqslant$ 99%), DVB (80%), AN (99%), azoisobutyronitrile (98%), octane ($\geqslant$99%), ethanol (99.8%), and methanol (99.9%) were obtained from Sigma-Aldrich. All solutions were prepared in de-ionized water (conductivity less than 0.1 μS/cm). Small amount of ethanol was added in order to facilitate BPA dissolution.

The MIP adsorbents were synthesized by bulk polymerization at 60 ˚C using the molar ratios given in Table 1. STY, AN, DVB, octane, and BPA were mixed and after addition of azoisobutyronitrile (1% wt.) reaction was conducted for 48 h. Bisphenol was added to obtain 5% and 10% wt. concentration in relation to monomers. After polymerization, blocks were ground and sieved to an average particle size of 90 mm. Finally, the sorbents were Soxhlet extracted with methanol for 24 h and dried.

BET surface areas for the adsorbents were measured using N_2 adsorption (Sorptomatic 1900 FISONS) and the results are listed in Table 1.

2.2. Methods

2.2.1. Adsorption isotherm measurements

Adsorption isotherms of BPA were measured by equilibration in separate batches. All measurements were made at room temperature ($T = 20–22$ ˚C) in aqueous solutions containing 0.5 mol/L of ethanol. A constant amount of the adsorbent (about 0.2 g) was weighed in glass vials containing different concentrations of BPA. The liquid volume of all samples was 20 mL. The samples were shaken at room temperature for at least 48 h. BPA concentrations were determined by UV–vis spectrometry (JASCO V530) at wavelength of 276 nm. The adsorbed amount was calculated from the change in the solution concentration. The values are given per unit weight of dry adsorbent. All samples were analyzed at least twice and the duplicate determinations agreed within 5%.

2.2.2. Adsorption kinetics measurements

Binding kinetics of BPA was measured at room temperature in a batch system with a liquid volume of 500 mL. Samples were taken from the solution and the BPA concentrations were determined by UV–vis spectroscopy. Mixing rate was 600 min^{-1}. The adsorption rate of BPA was expressed as the fractional uptake, F_a, defined in Eq. (1).

$$F_a = \frac{q_i(t) - q_i^0}{q_i^\infty - q_i^0} \tag{1}$$

In Eq. (1), $q(t)$ is the amount bound sorbate at time t, while q^0 and q^∞ are the values at $t = 0$ and at equilibrium, respectively.

2.2.3. Adsorption–microfiltration hybrid measurements

Dynamic adsorption was determined using adsorption–microfiltration hybrid system as described earlier [19], [22]. Experiments were carried out at room temperature using the experimental setup shown in Fig. 2.

Table 1
Synthesis and specific surface areas of the MIP adsorbents

Name	STY, mmol	AN, mmol	DVB, mmol	Octane, mmol	BPA, % wt.	Specific surface area, m^2/g
AN0	87.3	0	14.0	49.2	0	161
AN0-BPA5	87.3	0	14.0	49.2	5	175
AN0-BPA10	87.3	0	14.0	49.2	10	154
AN1	69.8	30.5	14.0	49.2	0	108
AN1-BPA5	69.8	30.5	14.0	49.2	5	112
AN1-BPA10	69.8	30.5	14.0	49.2	10	134
AN2	52.4	61.1	14.0	49.2	0	89
AN2-BPA5	52.4	61.1	14.0	49.2	5	112
AN2-BPA10	52.4	61.1	14.0	49.2	10	106

The system consists of a continuous stirred tank (CSTR) with recirculation through the membrane module and of the feed tanks for the BPA solutions and the adsorbent suspension. The hollow-fiber membrane module contains two polypropylene membranes with diameter of 0.5 mm, wall thickness 200 μm, pore diameter 0.4 μm, and length 30 cm. Initially, 250 mL of 0.2 mM BPA solution was put in tank A and the recirculation loop. At $t = 0$, 0.5 g of adsorbent was added to tank A and pumping of the adsorbent suspension through the system was started. At the same time the fresh BPA solution was added by siphoning from tank C. Feed flow rate of the adsorbent suspension was 3.1 mL/min and the adsorbent concentration was 1.8 g/L. The loaded adsorbent was removed from the system at the same rate. Hydrostatic pressure generated microfiltration flow and permeate flow rate was 1.5 mL/min.

3. Theory

As discussed elsewhere [22], mass balance for BPA in the hybrid system can be written as shown in Eq. (2). Dilute PAC dispersions were used and, therefore, dispersion volume was assumed equal to the liquid volume.

$$\frac{d(V_L c)}{dt} + \frac{d(m_{ads} q_{av})}{dt} = \dot{V}_{in} c^{in} - \dot{V}_{ads}^{out}\left(c + \frac{m_{ads} q_{av}}{V_L}\right) - \dot{V}_{perm} c^{perm} \qquad (2)$$

Here, V_L is the liquid volume in the stirred tank and the recirculation loop, c is solution concentration

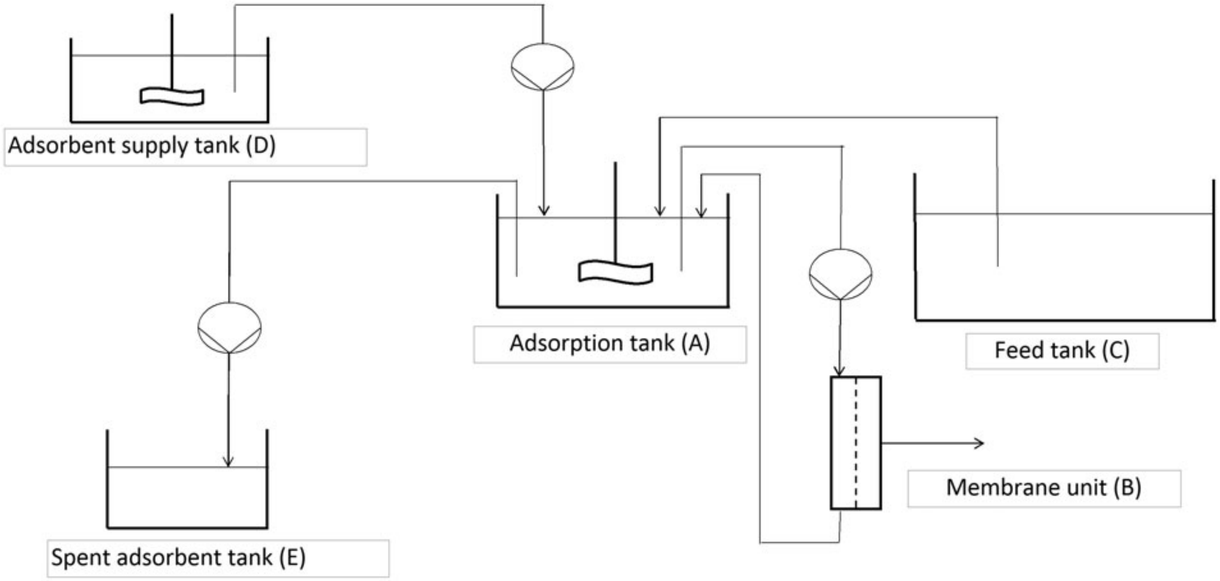

Fig. 2. Experimental setup of the adsorption-membrane hybrid system [19].

of BPA, and t is time. Volumetric flow rates of the feed, adsorbent removal, and permeate streams are given by $\dot{V}_{\mathrm{in}}$, $\dot{V}_{\mathrm{ads}}^{\mathrm{out}}$, and $\dot{V}_{\mathrm{perm}}$, respectively. The feed concentration is c^{in} and the subscript "ads" refers to the adsorbent. In batch kinetic experiments the right-hand side of Eq. (2) equals 0, and V_{L} and m_{ads} remain constants.

In the hybrid runs, the adsorbent added in tank A at $t=0$ and the adsorbent added continuously from tank D are considered separately. For the continuous mode, the average amount adsorbed at time t by particles having different residence times τ, $q_{\mathrm{av,i}}$, is obtained by averaging over the adsorbent particles and by taking into account the residence time distribution (RTD) as shown in Eq. (3). R is the average radius of the adsorbent particles, q is the local adsorbed amount, and $E(t,\tau)$ is the RTD in the hybrid system.

$$\begin{aligned} q_{\mathrm{av}}(t) &= \int_0^{\mathrm{t}} E(t,\tau)\,\bar{q}(t,\tau)d\tau \\ \bar{q}(t,\tau) &= \tfrac{3}{R}\int_0^{\mathrm{R}} q(t,\tau,r)dr \end{aligned} \tag{3}$$

Function $E(t,\tau)$ was evaluated experimentally [22] and the result was expressed as a polynomial shown in Eq. (4), where t is given in minutes. The adsorbent particles added at $t=0$ have same residence time and, therefore, $q_{\mathrm{av}} = \bar{q}$.

$$\begin{aligned} E(t) &= (0.060 + 5.38\cdot 10^{-3}t - 5.02\cdot 10^{-5}t^2 \\ &\quad + 1.46\cdot 10^{-7}t^3 - 1.38\cdot 10^{-10}t^4)/\tau_{\mathrm{hydr}}\tau_{\mathrm{hydr}} \\ &= \frac{V_{\mathrm{L}}^0}{\dot{V}_{\mathrm{ads}}^{\mathrm{in}}} \end{aligned} \tag{4}$$

The volume-averaged loading of BPA, $\bar{q}(t,\tau)$, was calculated using the particle mass balance shown in Eq. (5). It is assumed here that the adsorbent particles can be treated as spherical and pore diffusion is the rate-controlling step. The pore diffusion coefficient is represented by D_{p}. In Eq. (5), c_{p} is pore concentration of BPA, r_{ads} is adsorbent density, e_{p} is particle porosity, and r is radial coordinate.

$$\varepsilon_{\mathrm{p}}\tfrac{\partial c_{\mathrm{p}}}{\partial t} + \rho_{\mathrm{ads}}\tfrac{\partial q}{\partial t} = \tfrac{\varepsilon_{\mathrm{p}}}{r^2}\frac{\partial}{\partial r}\left[r^2 D_{\mathrm{p}}\frac{\partial c_{\mathrm{p}}}{\partial r}\right] \tag{5}$$

Equilibrium is assumed to be established between the pore solution and the adsorbent surface, and c_{p} and q are related by Langmuir isotherm shown in Eq. (6).

$$q = \tfrac{q_{\max}K_{\mathrm{L}}c_{\mathrm{p}}}{1+K_{\mathrm{L}}c_{\mathrm{p}}} \tag{6}$$

Various mathematical transformations of the Langmuir isotherm, e.g. semi-reciprocal [23], double-reciprocal [24], and Scatchard [25], have been presented in the literature. Because Scatchard plot analysis is most suitable for analyzing the affinities of binding sites in a particular adsorption process [26], it has been used in the present study. Scatchard equation is shown in Eq. (7). When q/c is plotted as function of q, the effect of concentration on the shape of Scatchard plot is theoretically eliminated [26].

$$\frac{q}{c} = q_{\max}K_{\mathrm{a}} - qK_{\mathrm{a}} \tag{7}$$

Langmuir isotherm was also used to describe adsorption equilibrium of BPA in the membrane. The membrane unit was considered as a non-steady CSTR and the mass balance for BPA becomes thus as follows:

$$V_{\mathrm{M}}\tfrac{dc^{\mathrm{perm}}}{dt} + A_{\mathrm{M}}\tfrac{dq^{\mathrm{M}}}{dt} = \dot{V}_{\mathrm{perm}}(c - c^{\mathrm{perm}}) \tag{8}$$

Here, $c_{\mathrm{i}}{}^{\mathrm{perm}}$ is the effluent concentration of the hybrid system, A_{M} is the membrane area, and V_{M} is the liquid volume in the membrane unit. Linear dependence of the permeate flow rate, $\dot{V}_{\mathrm{perm}}$, on pressure was assumed.

Finally, balance equations for the solution volume and adsorbent mass are given in Eq. (9), where d_{A} and d_{C} represent diameter of tanks A and C, respectively.

$$\begin{aligned} \frac{dV_{\mathrm{L}}}{dt} &= \frac{d_{\mathrm{A}}^2}{d_{\mathrm{A}}^2 + d_{\mathrm{C}}^2}(\dot{V}_{\mathrm{ads}}^{\mathrm{in}} - \dot{V}_{\mathrm{perm}} - \dot{V}_{\mathrm{ads}}^{\mathrm{out}}) \\ \frac{dm_{\mathrm{ads}}}{dt} &= \dot{V}_{\mathrm{ads}}^{\mathrm{in}}C_{\mathrm{ads}}^0 - \dot{V}_{\mathrm{ads}}^{\mathrm{out}}(\tfrac{m_{\mathrm{ads}}}{V_{\mathrm{L}}}) \end{aligned} \tag{9}$$

Calculations:

Eq. (5) was solved using a lumped concentration variable, $z = c_{\mathrm{p}} + \rho_{\mathrm{ads}}\, q/e_{\mathrm{p}}$, and the method of lines [27]. Resin density, which here means the solid content in the water-filled adsorbent, was 0.70 g/L and the resin porosity was 0.35. ODE's were solved by means of the DVODE package [28]. Initial and boundary conditions for the batch and hybrid runs were as follows. Here c^0 and c^{in} refer to the initial and feed concentrations of BPA in the batch and hybrid experiments, respectively.

Batch:

$t<0: c = 0, q = 0$

$t \geq 0: c = c^0, q = f(c_{\mathrm{p}})$

$$r = 0: \frac{\partial c_{\mathrm{p}}}{\partial_{\mathrm{r}}} = 0$$

$$r = d_p/2 : \frac{\partial c_p}{\partial_r} = \frac{6\varepsilon_p k_f}{d_p}(c - c_p)$$

Hybrid:

$$t<0 : c = 0, q = 0, c^{\text{perm}} = 0, V = V_L^0$$

$$t \geq 0 : c = c^{\text{in}}, q = f(c_p)$$

$$r = 0 : \frac{\partial c_p}{\partial_r} = 0$$

$$r = d_p/2 : \frac{\partial c_p}{\partial_r} = \frac{6\varepsilon_p k_f}{d_p}(c - c_p)$$

The film mass transfer coefficient, k_f, was estimated from the correlation of Nagata and Nishikawa [29] applicable for small particles.

4. Results and discussion

4.1. Equilibrium adsorption of BPA

In this study, we have investigated two methods to enhance BPA adsorption on the PS-DVB matrix. First, AN was co-polymerized with STY and DVB in order to introduce more specific interactions with BPA. The nitrile group of AN has a high dipole moment and can possibly interact with the polar phenolic groups of BPA. Secondly, the polymer matrix was imprinted with BPA to create adsorption sites of high specifity. Combination of these methods should result in very high affinity for BPA, thus allowing its removal to extremely low concentrations.

Adsorption isotherms of BPA in AN0, AN1, and AN2 prepared in the presence of different amounts of BPA template are shown in Fig. 3. Compositions of the adsorbents are shown in Table 1. Adsorption isotherms were correlated using single-component Langmuir equation (Eq. (6)). The calculated values are shown as solid lines (Fig. 3) and the estimated parameters are given in Table 2. Although the most common model to explain adsorption isotherms of BPA for MIP adsorbents is Freundlich equation [6], Langmuir isotherm was found in this work to give best correlation with the experimental isotherms.

Fig. 3 and Table 2 show that the highest BPA adsorption capacity was attained in cases where no AN was added. When the content of AN was zero, the capacities of the materials were about 10 times higher than in the syntheses with AN. The decrease of $q_{\max}$ is partly due to decrease of the specific surface area with increasing AN content in the polymer matrix (Table 1). For AN2, this effect explains about half of the decrease and other factors must also be

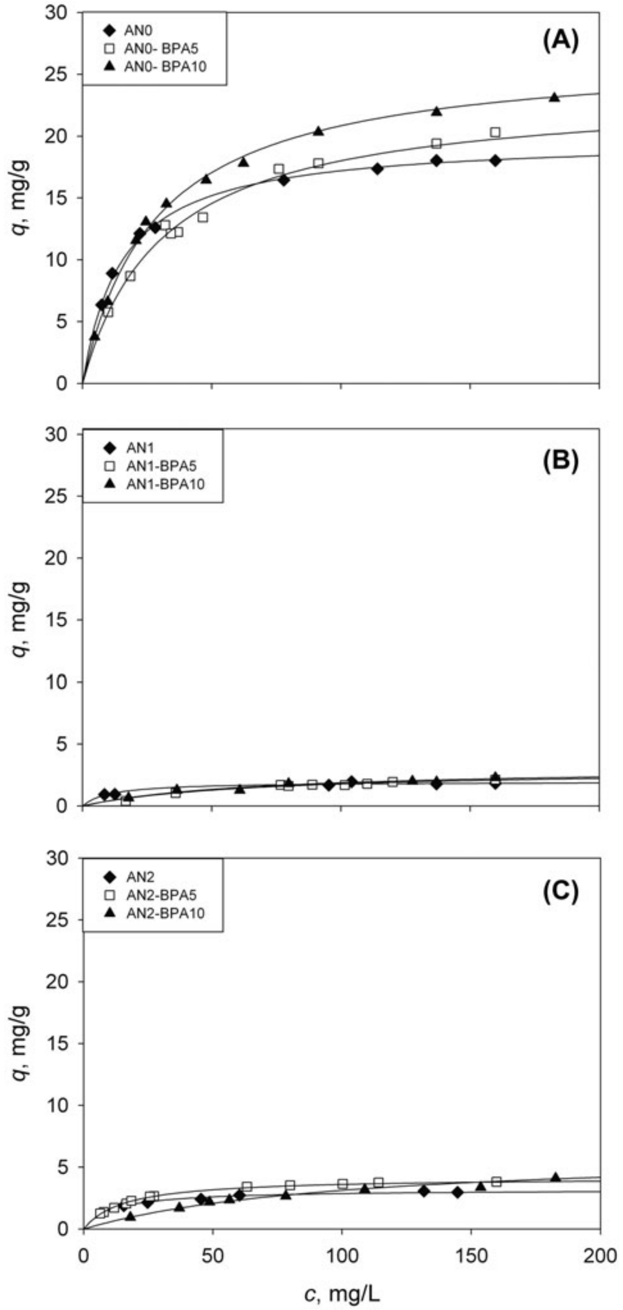

Fig. 3. Adsorption isotherms of BPA by AN0 (A), AN1 (B), and AN2 (C) in presence of BPA, in relation to the styrene 0% (diamonds), 5% (squares), and 10% (triangles). Compositions of the adsorbents are shown in Table 1. The solid lines were calculated using Langmuir equation.

Table 2
Langmuir isotherm parameters for BPA adsorption on the studied adsorbents at room temperature

	Langmuir			Scatchard		
Name	K_L, mL/mol	q_{max}, mg/g	R^2, –	K_a, mL/mol	q_{max}, mg/g	R^2, –
AN0	14.9	19.8	0.996	15.4	19.6	0.988
AN0-BPA5	7.3	23.6	0.994	6.9	24.2	0.966
AN0-BPA10	8.0	26.8	0.999	8.1	26.5	0.988
AN1	21.6	1.94	0.996	–	–	–
AN1-BPA5	3.5	2.93	0.996	–	–	–
AN1-BPA10	3.4	3.11	0.966	–	–	–
AN2	20.2	3.19	0.971	–	–	–
AN2-BPA5	14.6	4.17	0.996	–	–	–
AN2-BPA10	2.2	6.33	1.000	–	–	–

– Not calculated.

considered. The sorption strength characterized by K_L is somewhat higher for AN2 than for AN0. It seems, therefore, possible that adsorption on the co-polymer surface is more demanding and each BPA molecule may require more surface area than in the absence of AN. The situation is further complicated by uneven distribution of the STY and AN segments between surface and bulk. No analysis of the surface phase was attempted in this study but Adao et al. [30] have reported that in SAN co-polymers, low-energy styrene segments are concentrated on the surface phase.

Interactions between BPA and the adsorbents were studied by means of the Scatchard analysis (Eq. (7)). The data for materials AN0, AN0-BPA5, and AN0-BPA10 are shown in Fig. 4. As can be seen, all plots are decreasing linearly and there can be seen only one linear region. This means that in these three materials, there is only one type of binding sites and no clear indication of high-affinity sites due to imprinting was found [26]. Furthermore, the adsorption parameters calculated using the classical Langmuir equation (Eq. (6)) and the Scatchard transform (Eq. (7)) match closely as expected (see Table 2).

Results in Fig. 3 and Table 2 also show the positive effect of BPA imprinting on the maximum adsorption capacity q_{max}. When AN0 was prepared in the presence of both 5 and 10% BPA template, the uptake capacity increased of 15 and 30%, respectively, when compared to template-free sorbent. The maximum BPA capacity of 27 mg/g, obtained using 10% BPA template (AN0-BPA10), is quite high when compared with capacities of imprinted materials reported in literature [1,3]. However, Jiang et al. [10] have reported even much higher capacity, 68.9 mg/g using sol-gel surface imprinting technique. For AN1 and AN2, the positive effect of BPA template is also discernible in spite of the much lower maximum capacity q_{max}.

The higher adsorption capacity of the imprinted materials is possibly due to structural effects caused by the added template. Increase of the specific surface area in the presence of the template (Table 1) explains part of the capacity increase but changes observed in the K_L values mentioned in Table 2 appear to be a more important factor. However, origin of such negative imprinting effect is not clear.

In conclusion, using AN as a co-monomer in synthesis of BPA imprinted materials, the specific surface area of the materials decreases and the BPA adsorption capacity is much lower than in materials with no AN. On the other hand, a positive effect on adsorption capacity is achieved by adding BPA as template. However, according to the Scatchard analysis (Fig. 4) only one type binding sites in the materials exists and the effect is due to structural effects caused by the added BPA.

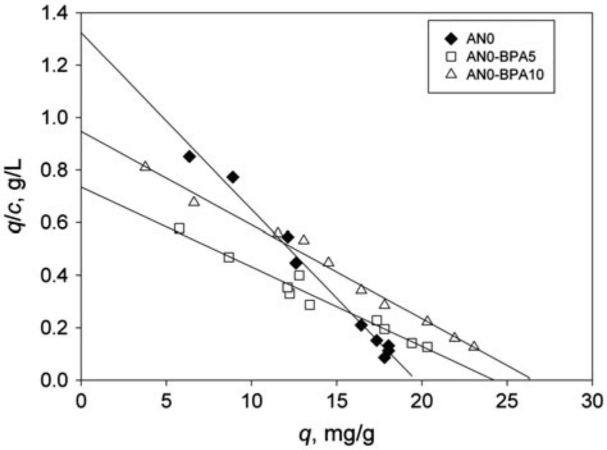

Fig. 4. Scatchard plots by AN0 in presence of BPA 0% (diamonds), 5% (squares), and 10% (triangles). Compositions of the adsorbents are shown in Table 1.

4.2. Adsorption kinetics of BPA

According to results shown in Chapter 4.1, the best material for removal of BPA is AN0-BPA10 and it was chosen for measurements with the adsorption–microfiltration hybrid system. Before applying the model illustrated in Chapter 3 to the hybrid system, the mass transfer parameters were first determined for this material. For this purpose, BPA adsorption rate was measured in a batch experiment at room temperature using an initial BPA concentration of 23 mg/L. The experimental uptake curve is shown in Fig. 5 along with the calculated values given as continuous line. The latter was obtained from Eqs. (2), (5), and (6). The fractional uptake is defined as shown in Eq. (1). The calculated curve was obtained from Eqs. (2), (5), and (6) using a pore diffusion coefficient $D_p = 2 \times 10^{-10}\,\mathrm{m^2/s}$ and the equilibrium parameters listed in Table 2. D_p was estimated by trial-and-error method and using a film mass transfer coefficient, $k_f = 6 \times 10^{-5}\,\mathrm{m/s}$.

Results in Fig. 5 show that 50% uptake was attained in about 8 min. Moreover, the experimental adsorption curve can be described reasonably well with the pore-diffusion model. When comparing the estimated D_p with the reported bulk diffusion coefficient, $D_{BPA} = 5.9 \times 10^{-10}\,\mathrm{m^2/s}$ [31], a tortuosity factor of about 3 is obtained.

4.3. Removal of BPA using adsorption–microfiltration hybrid system

Experimental data with the hybrid system were measured using the AN0-BPA10 adsorbent and BPA feed concentration of 46 mg/L. Adsorbent concentration in tank D was 1.8 g/L and the amount added at $t = 0$ was 0.5 g. The operation conditions were selected for testing of the model parameters rather than for optimal removal of BPA.

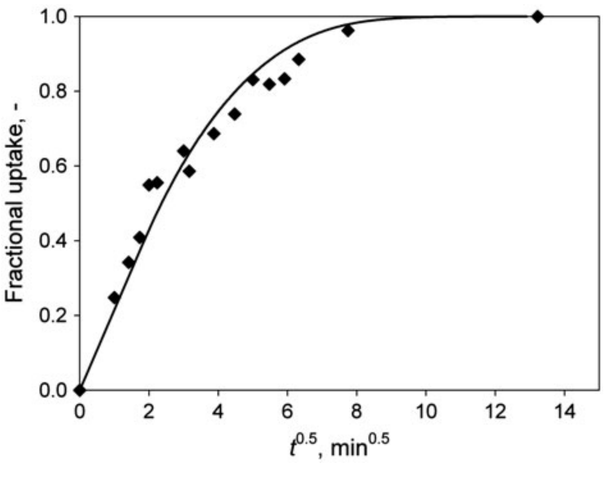

Fig. 5. Adsorption kinetics of BPA in AN0-BPA10 at room temperature. Solid line represents calculated values.

The measured BPA concentration in the permeate stream is depicted as symbols in Fig. 6. It is evident from the experimental data that after a relatively long transient period, the permeate concentration levels off at about 11 mg/L. It should be noted, however, that this is not a true steady-state value, because no such state is attained in the present system. The data were simulated using the equilibrium and mass transfer parameters determined in previous sections and the calculated data are shown as solid line in Fig. 6. In hybrid runs, the film mass transfer coefficient was estimated as $k_f = 3 \times 10^{-5}\,\mathrm{m/s}$. The model calculations agree rather well with the measured data indicating that the various contributions in the hybrid system are adequately accounted for.

The model calculations were used to investigate influence of some operation parameters on the BPA removal efficiency in the one-stage process. Assuming that the feed rate and concentration are kept constant, BPA removal can be improved by increasing the adsorbent concentration in tank D or the adsorbent feed flow rate. Effect of these variables is illustrated in Figs. 6 and 7, respectively. The continuous lines represent the calculated outlet concentrations of BPA in membrane module.

As can be seen from Fig. 6 if the feed concentration of the AN0-BPA10 adsorbent is 1.8 g/L, only 78% BPA can be removed. Increase in the concentration of the adsorbent feed stream lowers effectively the final BPA outlet concentration. If a 97% removal is wanted,

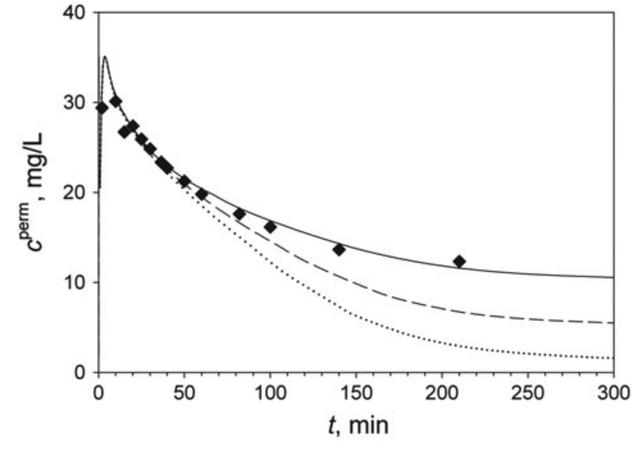

Fig. 6. Effect of adsorbent concentration on removal of BPA using adsorption–microfiltration hybrid system. Adsorbent AN0-BPA10, $c_{BPA} = 46\,\mathrm{mg/L}$, T = rt. Symbols are experimental data and lines are model calculations. $c_{ads} = 1.8\,\mathrm{g/L}$ (diamonds and solid line), 3.6 g/L (dashed line), and 5.4 g/L (dotted line).

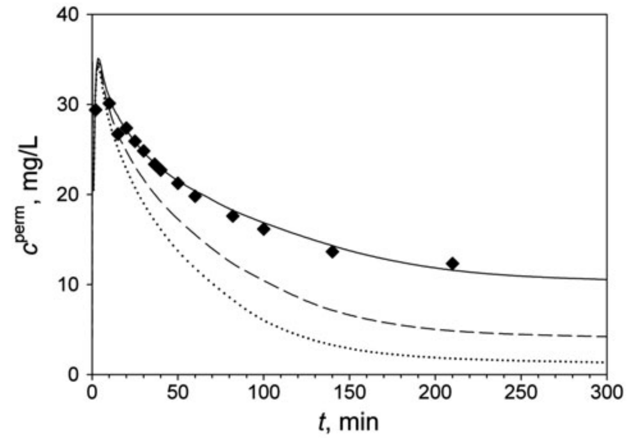

Fig. 7. Effect of adsorbent feed rate on removal of BPA, using adsorption–microfiltration hybrid system using AN0-BPA10. $c_{\text{BPA}} = 46\,\text{mg/L}$, $T = \text{rt}$. Symbols are experimental data and lines are model calculations. $\dot{V}_{\text{ads}}{}^{\text{in}} = 3.1\,\text{mL/min}$ (diamonds and solid line), 4.7 mL/min (dashed line), and 6.2 mL/min (dotted line).

an adsorbent concentration of 5.4 g/L is needed. In this case, BPA loading in the adsorbent becomes very low (about 4.6 g/kg) and a single-stage process is not reasonable. Simulation of multi-stage cascades is, however, beyond the scope of this paper.

In a similar way, flow rate of the adsorbent suspension has a strong impact on the removal of BPA in adsorption–microfiltration hybrid system (Fig. 7). According to the results, 78% of BPA is removed when the flow rate is 3.1 mL/min. If the flow rate is doubled, nearly 97% of BPA can be removed. At the same time, the transient period becomes shorter because of the dynamics of CSTR system. In Fig. 6, on the other hand, flow rates remain constant and the higher amount of adsorbent affects only the final BPA level. Consequently, improvement in BPA removal in the adsorption–microfiltration system is obtained more effectively by increasing the adsorbent flow rate than the adsorbent concentration.

5. Conclusions

The obtained results showed that incorporation of acrylonitrile to polymer matrix did not improve BPA adsorption properties. The best BPA uptake was achieved for sorbents without acrylonitrile. Furthermore, highest BPA adsorption capacity was noted for sorbents prepared with presence of 10% of BPA template. The presence of template in the reactant mixture did not result in creation of detectable amount of high affinity centers (expressed by K_a values) but increased the contents of the sorption sites.

In removal of BPA using adsorption–microfiltration hybrid system, the most efficient BPA separation can be achieved by adjusting the flow rate of fresh adsorbent. The obtained results show that the higher was the flow rate of fresh adsorbent, the faster was the apparent steady-state achievement.

Acknowledgments

Financial support from the Research Foundation of Lappeenranta University of Technology, Emil Aaltonen Foundation and Centre for International Mobility CIMO are gratefully acknowledged. MB appreciates financial support of Polish Ministry of Science and High Education through statutory subsidy for Faculty of Chemistry, Wrocław University of Technology - Grant No 344045/Z0309.

Nomenclature

A — area, m^2
c — concentration, mg/L
E — residence time distribution, 1/s
F_a — fractional uptake, -
d — diameter, m
D_p — pore diffusion coefficient, m^2/s
k_f — film mass transfer coefficient, m/s
K_a — affinity coefficient, mL/mol
K_L — Langmuir parameter, mL/mol
m — mass, g
q — adsorbed amount, mg/g
$\bar{q}$ — volume-averaged value of q, mg/g
$q_{\max}$ — adsorption capacity, mg/g
R_2 — regression coefficient, -
t — time, s or min
V — volume, L
$\dot{V}$ — volumetric flow rate, mL/min

Greek letters

t — residence time, s

Subscripts and superscripts

0 — initial value or fully mixed value
ads — adsorbent
av — average value
L — liquid phase
M — membrane
p — particle or pore
perm — permeate
s — surface

References

[1] T. Ikegami, T. Mukawa, H. Nariai, T. Takeuchi, Bisphenol A-recognition polymers prepared by covalent molecular imprinting, Anal. Chim. Acta 504 (2004) 131–135.

[2] C.A. Staples, P.B. Dorn, G.M. Klecka, S.T. O'Block, L.R. Harris, A review of the environmental fate, effects, and exposures of bisphenol A, Chemosphere 36 (1998) 2149–2173.

[3] K. Takeda, T. Kobayashi, Bisphenol A imprinted polymer adsorbents with selective recognition and binding characteristics, Sci. Technol. Adv. Mat. 6 (2005) 165–171.

[4] H. Fromme, T. Küchler, T. Otto, K. Pilz, J. Müller, A. Wenzel, Occurrence of phthalates and bisphenol A and F in the environment, Water Res. 36 (2002) 1429–1438.

[5] C.M. Markey, C.L. Michaelson, C. Sonnenschein, A.M. Soto, Alkyphenols and bisphenol A as environmental estrogens, in: M. Manfred (Ed.), The Handbook of Environmental Chemistry, Endocrine Disruptors, Part 1, Springer, Berlin, 2001 (Chapter 7), pp. 129–153.

[6] Z. Zhang, J. Hu, Selective removal of estrogenic compounds by molecular imprinted polymer (MIP), Water Res. 42 (2008) 4101–4108.

[7] I. Bautista-Toledo, M.A. Ferro-García, J. Rivera-Turilla, C. Moreno-Castilla, F.J. Vegasfernández, Bisphenol A removal from water by activated carbon. Effects of carbon characteristics and solution chemistry, Environ. Sci. Technol. 39 (2005) 6246–6250.

[8] K.J. Choi, S.G. Kim, C.W. Kim, S.H. Kim, Effects of activated crbon types and service life on removal of endocrine disrupting chemicals: Amitrol, nonylphenol, and bisphenol-A, Chemosphere 58 (2005) 1535–1545.

[9] S.A. Snyder, S. Adham, A.M. Redding, F.S. Cannon, J. DeCarolis, J. Oppenheimer, E.C. Wert, Y. Yoon, Role of membranes and activated carbon in the removal of endocrine disruptors and pharmaceuticals, Desalination 202 (2007) 156–181.

[10] X. Jiang, W. Tian, C. Zhao, H. Zhang, M. Liu, A novel sol–gel-material prepared by a surface imprinting technique for the selective solid-phase extraction of bisphenol A, Talanta 72 (2007) 119–125.

[11] T. Ikegami, W.-S. Lee, H. Nariai, T. Takeuchi, Synthetic polymers adsorbing bisphenol A and its analogues prepared by covalent molecular imprinting using bisphenol A dimethacrylate as a template molecule, Anal. Bioanal. Chem. 378 (2004) 1898–1902.

[12] R.D. Makote, S. Dai, Matrix-induced modification of imprinting effect for Cu^{2+} adsorption in hybrid silica matrices, Anal. Chim. Acta 435 (2001) 169–175.

[13] R. Gupta, R. Kumar, Molecular imprinting in sol–gel matrix, Biotechnol. Adv. 26 (2008) 533–547.

[14] M. Kempe, K. Mosbach, Molecular imprinting used for chiral separations, J. Chromatogr. A 694 (1995) 3–13.

[15] O. Ramström, R.J. Ansell, Molecular imprinting technology: Challenges and prospects for the future, Chirality 10 (1998) 195–209.

[16] L. Schweitz, L.I. Andersson, S. Nilsson, Molecular imprint-based stationary phases for capillary electrochromatography, J. Chromatogr. A 817 (1998) 5–13.

[17] J. Olsen, P. Martin, I.D. Wilson, Molecular imprints as sorbents for solid phase extraction: Potential and applications, Anal. Commun. 35 (1998) 13H–14H.

[18] L.I. Andersson, Molecular imprinting: Developments and applications in the analytical chemistry field, review, J. Chromatogr. B 745 (2000) 3–13.

[19] I. Yilmaz, N. Kabay, M. Bryjak, M. Yüksel, J. Wolska, A. Koltuniewicz, Study of submerged membrane-ion exchange hybrid process for boron removal, Desalination 198 (2006) 310–315.

[20] S. Khirani, P.J. Smith, M.-H. Manéro, R.B. Aim, S. Vigneswaran, Effect of periodic backwash in the submerged membrane adsorption hybrid system (SMAHS) for wastewater treatment, Desalination 191 (2006) 27–34.

[21] M. Bryjak, I. Duraj, Molecular imprinted membranes for removal of bisphenol A, Solvent Extr. Ion Exch. 29 (2011) 432–439.

[22] K. Laatikainen, M. Laatikainen, M. Bryjak, T. Sainio, H. Siren, Adsorption of bisphenol A from water-ethanol mixtures on pulverized activated carbon, Sep. Sci. Technol. submitted.

[23] O. Gezici, H. Kara, S. Yanık, H. Ayyildiz, S. Kucukkolbasi, Investigating sorption characteristics of copper ions onto insolubilized humic acid by using a continuously monitored solid phase extraction technique, Colloids Surf. A. 298 (2007) 129–138.

[24] L.A. Warren, F.G. Ferris, Continuum between sorption and precipitation of Fe(III) on microbial surfaces, Environ. Sci. Technol. 32 (1998) 2331–2337.

[25] G. Scatchard, The attractions of proteins for small molecules and ions, Ann. N.Y. Acad. Sci. 51 (1949) 660–672.

[26] O. Gezici, H. Kara, A. Ayar, M. Topkafa, Sorption behavior of Cu(II) ions on insolubilized humic acid under acidic conditions: an application of scatchard plot analysis in evaluating the pH dependence of specific and nonspecific bindings, Sep. Purif. Technol. 55 (2007) 132–139.

[27] W.E. Schiesser, The Numerical method of lines, Spatial differentiation (Chapter 3), 141, Academic Press, 1991, San Diego.

[28] A.C. Hindmarsh, in R.S: Stepleman (Ed.), Scientific computing, 1983, North-Holland, Amsterdam, p. 55.

[29] S. Nagata, M. Nishikawa, Mass transfer from suspended microparticles in agitated liquids, in: Proceedings of First Pacific Chemical Engineering Congress, The Society of Chemical Engineerings, Japan and The American Institute of Chemical Engineerings, Kyoto, Japan, 1972, p. 301.

[30] M.H. Adao, B.J. Saramago, A.C. Fernandes, Estimation of the Surface Properties of Styrene-Acrylonitrile Random Copolymers from Contact Angle Measurements, J. Coll. Interface Sci. 217 (1999) 94–106.

[31] Anon, http://www.gsi-net.com/en/publications/gsi-chemical-database/single/67.html, 2.2.2012.